

Efficient Subsampling for GNN Downstream Tasks

Author Name1

ABC@SAMPLE.COM and **Author Name2**

XYZ@SAMPLE.COM

Address

Editors: Hung-yi Lee and Tongliang Liu

Abstract

While Graph Neural Networks (GNNs) have shown significant promise for data integration using graph structures, methods to support subsampling graph data are lagging. To address this gap, in this paper, we propose a novel importance-based data subsampling framework. This framework strategically identifies inputs from a primary graph dataset based on their impact on the model’s learning of downstream tasks, such as graph or node classification. Our measure of impact is the predictive uncertainty of each data point. To ensure the subsample is well-representative of the original sample, we cluster them based on their learned graph representation. Finally, subsampling is performed from these identified clusters. The process favours selecting data points with greater prediction uncertainty, while preserving the diversity of the overall sample. We evaluate our approach using a multi-source, real-world dataset on child and youth mental health, comprising emergency department (ED) admissions and mental health questionnaire data. Our experimental results demonstrate that training a GNN with samples identified by the proposed framework yields a statistically significant improvement (on average, 10.13% improvement across metrics from the baseline approach) in predictive performance compared to training on a randomly selected subset of patients. The code is available at https://anonymous.4open.science/r/graph_subsampling-5343.

Keywords: Graph Subsampling; Multi-Dataset Data Integration; Uncertainty Quantification.

1. Introduction

Graph Neural Networks (GNNs) have emerged as a powerful class of deep learning models designed to handle data with complex relational structures. While GNNs have demonstrated strong potential for integrating data through graph-based representations, techniques for effectively subsampling graph data remain underdeveloped. An important application area of graph data subsampling is in medical AI, where data is often multi-modal and collected from diverse data stores. The following real-world case demonstrates the challenges of graph data subsampling.

The authors of this article, in collaboration with a clinical team, are designing a clinical decision support system for mental health using GNN where the relational structure arises from the electronic health records (EHRs) of the patients and their responses to mental health questionnaire, where the data collection scale is on the order of thousands. To improve the prediction performance of the network, the study also needs to collect audio data from a subset of patients on the order of a hundred, as the process of audio data collection is resource-intensive. As a result, finding patients who are well-representative of

36 the original patient data and at the same time will have the most influence on the network’s
 37 performance is a major challenge this research project is facing.

38 Several researchers have studied the problem of graph data subsampling with the goal
 39 of improving network performance ([Xu et al., 2023](#); [Jin et al., 2022](#); [Gupta et al., 2024](#);
 40 [Georgiev et al., 2023](#); [Jain et al., 2025](#)). These studies primarily focus on compressing graphs
 41 or sampling subgraphs, thereby reducing both dataset size and the size of individual graphs.
 42 However, graph compression is generally not applicable to diverse graph integration, where
 43 data originates from various data stores, such as EHRs and mental health questionnaires,
 44 each with its own distinct graph structure. Unlike graph compression, which aims to reduce
 45 the size of a graph, graph integration often seeks to construct larger, unified graphs. A
 46 promising approach with potential for graph data subsampling is coresets selection, which is
 47 primarily used in active learning. Coreset selection offers an approach to select informative
 48 samples from unlabeled data for human labelling, which can subsequently improve network
 49 performance ([Yoo and Kweon, 2019](#); [Katharopoulos and Fleuret, 2018](#)).

50 In this paper, we propose an efficient graph subsampling approach tailored for down-
 51 stream prediction tasks, such as graph classification. We are inspired by the coresets se-
 52 lection approach in identifying samples that are most influential for training a predictive
 53 GNN. We use the network’s prediction uncertainty as a metric for identifying samples that
 54 are highly informative for network training ([Katharopoulos and Fleuret, 2018](#); [Jeong et al.,](#)
 55 [2023](#); [Chen et al., 2024](#)). However, to improve efficiency, we employ self-distillation in the
 56 quantification of uncertainty. Self-distillation allows for the training of a multi-classifier
 57 GNN, thereby significantly reducing the computational costs of both training and infer-
 58 ence for uncertainty estimation ([Daneshvar and Samavi, 2025](#)). Selecting data points solely
 59 based on the highest uncertainty can lead to the undesirable outcome of mostly selecting
 60 outliers ([Katharopoulos and Fleuret, 2018](#); [Jeong et al., 2023](#); [Settles and Craven, 2008](#);
 61 [Chen et al., 2024](#)). To counter this problem and promote diversity among selected sam-
 62 ples, we utilize K-means clustering based on graph representations. Within each cluster,
 63 data points are further grouped into percentiles according to their uncertainty values. Our
 64 diversity-enabled grouping strategy ensures the inclusion of samples across the full range
 65 of uncertainty, preventing bias towards extreme outliers. Ultimately, samples are selected
 66 with a weighted emphasis on those exhibiting higher prediction uncertainty.

67 The key contributions of this paper are as follows. First, we propose a diversity-enabled
 68 subsampling method for GNNs specifically designed for graph classification—an underex-
 69 plored direction, particularly in the context of heterogeneous graphs. Second, our method
 70 leverages self-distillation to train a multi-classifier GNN, followed by uncertainty quantifi-
 71 cation, substantially reducing the computational cost typically associated with uncertainty-
 72 based subsampling. Third, we empirically demonstrate that our framework effectively se-
 73 lects representative samples from a primary dataset to augment with a secondary one,
 74 thereby improving training performance in scenarios involving diverse data integration un-
 75 der limited-data conditions.

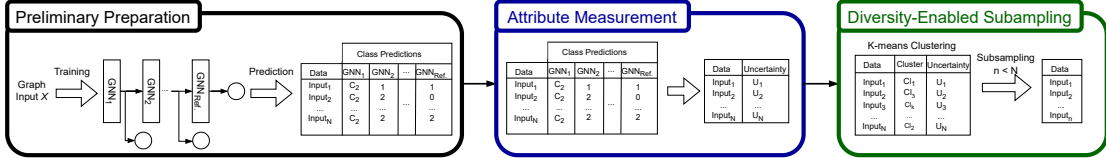


Figure 1: Overview of the proposed subsampling approach.

76 2. Methodology

77 2.1. Problem Setup

78 Our proposed approach is inspired by *coreset selection*, a technique primarily used in active
 79 learning to efficiently select representative samples from an unlabeled dataset for human
 80 experts to label (Yoo and Kweon, 2019). By adopting similar principles, we aim to pro-
 81 pose a subsampling methodology for graphs that selects samples highly relevant to a given
 82 downstream task, such as graph classification, thereby making the sample more effective for
 83 GNN training.

84 There are three approaches of coreset selection: (1) uncertainty-based, (2) diversity-
 85 based, and (3) approaches based on expected changes in the network (Yoo and Kweon,
 86 2019). The uncertainty-based approaches utilize the quantified uncertainty of the data
 87 points to select samples with higher uncertainty. Diversity-based approaches select di-
 88 verse samples to represent the underlying distribution of the data. Finally, the approaches
 89 based on the expected changes in the network select samples with greater impact on net-
 90 work parameters or outputs (Yoo and Kweon, 2019). Key challenges in coreset selection
 91 include achieving computational efficiency, a common disadvantage of uncertainty-based
 92 approaches, and simultaneously ensuring sample diversity.

93 Our proposed approach addresses both key challenges in identifying the most influ-
 94 ential samples for network training. Specifically: (1) the method achieves computational
 95 efficiency in uncertainty quantification by utilizing only one network instead of multiple
 96 networks (deep ensemble) or multiple passes of the input through the same network (MC
 97 Dropout). Furthermore, (2) the subsampling strategy promotes diversity among samples
 98 by grouping the data based on their graph structure and sampling from all groups. As
 99 shown in Figure 1, the approach consists of three pipelines: (1) preliminary preparation
 100 (Section 2.2), (2) attribute measurement, in which we have chosen prediction uncertainty
 101 as the attribute (Section 2.3), and (3) diversity-enabled subsampling (Section 2.4). We use
 102 GNNs for graph classification throughout this work; however, the approach is generalizable
 103 to any classification task involving GNNs.

104 2.2. Preliminary Preparation

105 The goal of the preliminary preparation phase is to train a network that can be effectively
 106 utilized to quantify the prediction uncertainty for all data points. We utilize the *self-*
 107 *distillation* approach to train multiple GNN networks simultaneously. Self-distillation is a
 108 special case of knowledge distillation, where the same network serves as both the teacher
 109 and the student simultaneously, facilitating knowledge transfer within the network (Zhang

et al., 2022; Gou et al., 2021). Self-distillation is especially helpful when used with over-parameterized GNNs as it reduces the computational complexity of training multiple networks separately (Chen et al., 2021). We follow the same strategy as Zhang et al. (2022) by adding a classifier after each layer of the network and utilizing the deepest classifier as the teacher.

During training, each classifier learns to mimic the deepest classifier, i.e., the teacher. As a result, the training process involves reducing the total distillation loss, which is a combination of distillation loss and feature penalty (Zhang et al., 2022; Daneshvar and Samavi, 2025). The total distillation loss for all n training graphs can be defined as

$$L = \frac{1}{n} \sum_{i=1}^n L_{\text{dist}}^i + L_{\text{pen}}^i, \quad (1)$$

where L_{dist} and L_{pen} are the distillation loss and feature penalty respectively.

The distillation loss is the mean of layer-wise weighted sums of two components, cross-entropy and KL-divergence, and can be computed as

$$L_{\text{dis}}^i = \frac{1}{m} \sum_{l=1}^m \left((1 - \alpha_l) L_{\text{CE}_l}^i + \alpha_l L_{\text{KL}_l}^i \right), \quad (2)$$

where $\alpha_l \in [0, 1]$ is the imitation parameter for each classifier. The L_{CE} and L_{KL} are the cross-entropy of the classifier output at layer l with the true label, and the KL-divergence between the student's soft labels at layer l and the teacher's soft labels, respectively. The feature penalty can be computed as

$$L_{\text{pen}}^i = \frac{1}{m} \sum_{l=1}^m \lambda_l L_2(h_l^i, h_t^i), \quad (3)$$

where $\lambda_l > 0$ is the trade-off parameter for each classifier and L_2 is the squared ℓ_2 -norm loss. h_l^i and h_t^i are features extracted in layer l and features extracted by the teacher network, respectively. Both the imitation parameter and the trade-off parameter are set to zero for the teacher network.

To make predictions for all data points, we utilize K-fold cross-validation. As a result, each data point will be included in the test dataset exactly once. The predictions of the students and the teacher network are recorded for each data point in the test dataset, which will later be used to distinguish between hard and easy examples.

2.3. Attribute Measurement

During the attribute measurement phase, we utilize the previously trained network to quantify the prediction uncertainty of each data point in the dataset. A data point would be harder for the network to classify if the prediction of shallower classifiers, i.e., classifiers after shallower layers, don't match that of the deepest classifier (Zhang et al., 2022; Daneshvar and Samavi, 2025). This is because deeper classifiers utilize deeper feature extractors, providing them with more informative information. This is especially the case with GNNs, as deeper graph layers, i.e., deeper feature extractors, aggregate information from more distant nodes (Hamilton, 2020). To rank the samples based on how hard they are for the network

143 to classify, we utilize a metric proposed by [Daneshvar and Samavi \(2025\)](#) that captures dis-
144 agreement between predictions of each classifier. The disagreement between the classifiers'
145 predictions is referred to as the network's prediction uncertainty.

146 To quantify the network's prediction uncertainty, the metric utilizes a weighted disagree-
147 ment metric based on a normalized weighted Jensen–Shannon divergence (JSD) ([Daneshvar](#)
148 and [Samavi, 2025](#)). The uncertainty metric can be computed as

$$UC = \sum_{l=1}^m W(l) \times JSD(P_l || P_{teacher}), \quad (4)$$

149 where $W(l)$ is a bounded weight function ($1 \leq W(l) \leq 2$) that assigns a weight to layer l .
150 We utilize the same nonlinear weight function proposed by [Daneshvar and Samavi \(2025\)](#).

151 The goal of the weight function is to assign higher weights to classifiers based on their
152 depth relative to the deepest classifier. The weight of a classifier at layer l is computed by

$$W(l) = (-(\exp(D(l) - L)) + 2)^{\mathbb{1}_{\{y_l \neq y_{teacher}\}}}, \quad (5)$$

153 where L and $D(i)$ are the total number of network layers and classifier i 's distance from the
154 deepest layer, respectively. $\mathbb{1}$ is the indicator function, which returns one if the y_l differs
155 from $y_{teacher}$; otherwise, it returns zero. y_l and $y_{teacher}$ are the predicted class by the l th
156 classifier and the predicted class by the teacher classifier, respectively.

157 JSD can be computed as

$$JSD(P_l || P_{outcome}) = \frac{1}{2} \left(KL(P_l || M) + KL(P_{outcome} || M) \right), \quad (6)$$

158 where $M = \frac{1}{2}(P_l + P_{outcome})$ is a mixture distribution of P_l and $P_{outcome}$. JSD is bounded
159 ($0 \leq JSD \leq \log_b(2)$) as the mixture distribution helps with averaging and smoothing out
160 the values. The uncertainty quantification metric needs to be normalized. The upper bound
161 of UC for a network with m layers, including the teacher network, can be computed as

$$UC_{max} = \sum_{l=1}^{m-1} W(l) \times \log_e(2), \quad (7)$$

162 where \log_e is the natural logarithm and $W(l)$ computes layer l 's. Finally, the normalized
163 uncertainty metric can be computed as

$$UC_{norm} = \frac{UC}{UC_{max}}. \quad (8)$$

164 Algorithm 1 outlines the overall steps in quantifying the uncertainty of each data point. It
165 begins by training a network for each split (lines 2-6) and then quantifying the uncertainty
166 of the test set for each split (lines 7-11).

167 2.4. Diversity-Enabled Subsampling

168 The diversity-enabled subsampling phase ensures that the selected samples are not only rep-
169 resentative of the dataset but also more influential in training the final predictive network.

Algorithm 1: Computing uncertainty of all data points

Input: Graph data points X , a GNN network M , total number of layers l

Output: Prediction uncertainty of the data points U

```

1  $U \leftarrow \emptyset$ 
2 // Step 1: Split data using K-Fold Cross Validation.
3 foreach  $(trainSet, testSet) \in k\_fold(X)$  do
4   // Step 2: Train the network on trainSet.
5    $M \leftarrow train(M, trainSet)$ 
6   // Step 3: Compute uncertainty of testSet.
7   foreach  $testData \in testSet$  do
8      $u \leftarrow 0$ 
9      $u \leftarrow uncertainty(M, testData, l)$  // Compute uncertainty.
10     $U \leftarrow U \cup \{u\}$  // Add  $u$  to the set  $U$ 
11  end
12 end
13 return  $U$ 

```

170 If the subsampling strategy selects only from the data points with the highest uncertainty,
 171 we risk selecting only from the outliers (Jeong et al., 2023; Settles and Craven, 2008).
 172 Therefore, to promote diversity among samples, we will first group the graphs and then
 173 sample graphs proportional to the size of each group. We can utilize unsupervised learning
 174 to find hidden patterns in the data without the need for labelled data. One fundamental
 175 unsupervised learning approach is clustering. Clustering aims to group data samples based
 176 on similarity without requiring labelled data by finding hidden patterns that might exist
 177 in the data (Xu and Wunsch, 2005; Huang, 1998). The clustering algorithm will provide
 178 disjoint clusters, each containing data that is similar (Na et al., 2010). One of the widely
 179 used algorithms in clustering is the K-means clustering algorithm (MacQueen, 1967), which
 180 is known for its simplicity.

181 The clustering approach in K-means clustering begins by selecting k cluster centers,
 182 usually chosen randomly. Then the algorithm assigns each data point to a cluster based on
 183 its distance to the chosen centers. Euclidean distance is a widely used metric to compute the
 184 distance of each data point to the cluster centers (Xu and Wunsch, 2005; Na et al., 2010).
 185 The value of k is arbitrary and fixed at the beginning of the algorithm. After assigning
 186 each data point to a cluster, the algorithm recalculates the cluster centers by minimizing an
 187 objective function. The objective function reduces the distance of each item in the cluster
 188 to the cluster average (cluster center), and is computed as (Na et al., 2010):

$$E = \sum_{i=1}^k \sum_{x \in C_i} |x - \bar{x}|^2, \quad (9)$$

189 where C_i , x , and \bar{x} are cluster i , data point x in cluster C_i , and the average of cluster C_i
 190 respectively. The process is repeated until there is no change in the cluster centers.

191 In our approach, we utilize the graphs' information for clustering. Graphs are grouped
 192 based on their graph representation. To this end, the graph representations created by
 193 the teacher network are utilized. The intuition behind grouping graphs based on their

representations is to ensure the sample is representative of the underlying data distribution while taking the graph structure into account.

The sum of the squared distances of samples to their closest cluster center, also known as inertia, is used to optimize the number of clusters (k). However, having too many clusters will result in poor subsampling, as there is a risk of outliers being assigned to the same cluster, and fewer data points in each cluster, resulting in a sample that is not representative of the dataset. Therefore, k should satisfy two conditions: (1) k should be a small number, i.e., limited number of cluster, and (2) the drop in the sum of the squared distances of samples to their closest cluster center computed with k clusters, should be significant compared to having only one cluster.

To reduce the risk of only selecting outliers in each cluster, the framework groups graphs in each cluster into four percentiles based on the uncertainty values computed by Equation (8), sorted in descending order, 0-25%, 25-50%, 50-75%, and 75-100%. The approach samples the same number of graphs from each cluster with an emphasis on the harder examples, i.e., 50-75% and 75-100% percentiles. To achieve this, in each cluster, random sampling is performed as follows: 45% of samples are drawn from the 75-100% percentile range, 30% from 50-75%, 15% from 25-50%, and 10% from 0-25%. Algorithm 2 outlines the subsampling strategy. It starts by grouping the graphs into k clusters using individual graphs (line 2). Then, for each group, samples will be chosen from each percentile with a focus on samples with higher uncertainty, i.e., upper percentiles, proportionate to the size of the cluster (lines 5-10).

Algorithm 2: Subsampling data points with higher uncertainty

Input: Graph representations provided by the teacher network G_{rep} , uncertainty of samples U , number of clusters k , and number of samples needed m

Output: Subset of the data points X' with higher uncertainty

```

1 // Step 1: Grouping graphs.
2 groups = k_means( $G_{rep}$ ,  $k$ )
3 // Step 2: Select a subsample of size  $m$ .
4  $X' \leftarrow \emptyset$ 
5 foreach group  $\in$  groups do
6    $n = round\left(\left(size(group)/size(X)\right) * m\right)$  // Samples needed from the group.
7   foreach  $(p_1, p_2, r) \in \{(0, 25, 0.1), (25, 50, 0.15), (50, 75, 0.3), (75, 100, 0.45)\}$  do
8      $X' \leftarrow X' \cup subsample\left(percentile(U, group, p_1, p_2), round(r * n)\right)$ 
9   end
10 end
11 return  $X'$ 

```

3. Experimental Evaluations

The proposed framework identifies and selects samples that provide superior utility for network training compared to random sampling. We assess the impact of our importance-based subsampling method on network performance, comparing it directly with random sampling. To do so, we evaluate the performance of an identical network trained under

220 three conditions: (1) on the entire dataset using K-fold cross-validation, (2) on randomly
 221 sampled data, and (3) on data sampled using the proposed framework. We anticipate ob-
 222 serving improved network performance when training with the limited data selected by our
 223 subsampling framework, compared to random sampling, and achieving comparable perfor-
 224 mance to training the network on all the training data.

225 3.1. Experimental Setup

226 **Dataset:** We have utilized two linked datasets containing data from medical health records
 227 and mental health questionnaires from real-world patients. The prediction task involves de-
 228 termining whether a patient will be admitted to the emergency department (ED) within
 229 180 days of completing the mental health questionnaire. The datasets comprise ED vis-
 230 its of 1,086 unique patients, along with their responses to the mental health outpatient
 231 questionnaire. There are 281 patients who have visited the ED within 180 days of their
 232 initial outpatient visit. To address dataset imbalance, we balanced the "Not Admitted" and
 233 "Admitted" groups by repeated undersampling the former to 281 patients. We utilized the
 234 available information to create a graph for each patient based on their medical history. We
 235 then utilized the mental health questionnaire responses to integrate additional data into
 236 each patient's graph. Appendix A provides more details on the dataset and the generated
 237 graph for each patient.

238 **Network:** We utilized two networks. The first network is a multi-classifier GNN, used
 239 by the subsampling framework to sample patients from the main dataset, i.e., the medical
 240 records dataset, trained using the self-distillation approach. The network consists of three
 241 GraphConv (Morris et al., 2021) layers, followed by a ReLU activation function and a batch
 242 normalization layer. A final readout layer is applied before each classifier, which consists of
 243 a global mean pooling layer. The purpose of utilizing a readout layer is to combine node
 244 representations into a single, final graph representation for use in graph classification. The
 245 network is trained on the same 180-day ED admission prediction task. It is worth noting
 246 that the first network is only utilized for uncertainty quantification; therefore, the network's
 247 performance is not a concern.

248 The second network utilizes the augmented patient graph, generated by integrating
 249 information from both datasets, to predict whether a patient would be admitted to the
 250 ED within 180 days of their initial mental health assessment. The network consists of
 251 a single layer of GraphConv (Morris et al., 2021), followed by similar ReLU and batch
 252 normalization layers. A similar readout layer is applied to the node representations to
 253 create a graph representation, which is then fed to the classifier.

254 **Training and Hardware Specifications:** All networks were implemented using Python
 255 version 3.9 and PyTorch version 1.13.1. The networks have been trained on a GPU (NVIDIA
 256 GeForce RTX 3050) with CUDA version 12.5. For optimization, we used Adam Optimizer.

257 3.2. Results and Discussion

258 To select a suitable value for k , we employed the *Elbow Method*. During each iteration, we
 259 used 33% of the data to fit a K-means clustering model and computed the inertia. Figure 2
 260 illustrates how different values of k ($1 \leq k \leq 20$) affect the inertia. As can be observed, $k =$

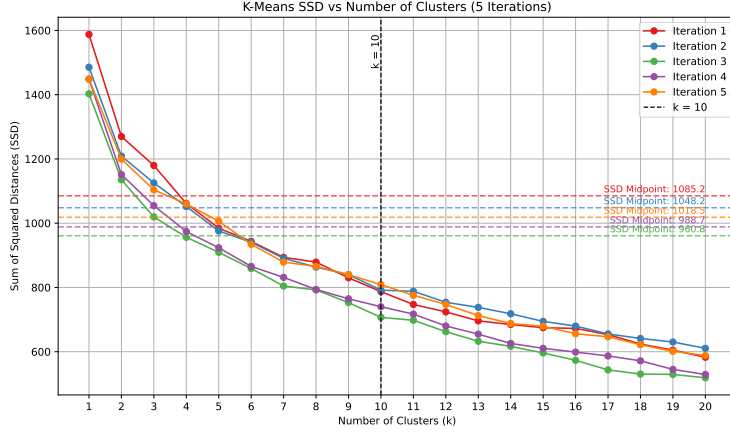


Figure 2: Candidate k versus sum of squared distances of samples to their cluster center, repeated for 5 iterations.

10 represents an 'elbow' point where the rate of decrease in inertia significantly diminishes. This observation was further validated by experimentally evaluating the effect of different k values on the overall subsampling framework. As shown in Table 1, increasing the number of clusters from 5 to 10 results in improved performance; however, performance decreases as the number of clusters approaches 20. The decline in performance occurs because a larger number of clusters can reduce the number of samples in each cluster, thereby increasing the risk of selecting more outliers and diminishing overall sample diversity. Thus, $k = 10$ yields the best performance among other candidates, as it (1) is small enough for computational efficiency yet large enough to provide sufficient diversity, and (2) substantially reduces the clustering error (by more than half), satisfying both conditions for selecting k as discussed in Section 2.4.

Table 2 shows the performance of the network. The same number of samples was selected for both the random sampling and the proposed framework (roughly 278 samples). Additionally, we trained the same GNN network without subsampling to compare the performance of the network trained with and without subsampling. The GNN network takes the augmented patient graph as input and predicts whether a patient would be at risk of admission to the ED within 180 days of their initial mental health assessment. We have measured accuracy, ROC AUC, precision, recall, and F1 score to compare the performance

Table 1: Comparison of different values of k on final network performance.

Number of Clusters	Accuracy	ROC AUC	F1 Score
5	0.5 ± 0.03	0.55 ± 0.06	0.51 ± 0.05
10	0.61 ± 0.04	0.63 ± 0.04	0.64 ± 0.03
15	0.52 ± 0.08	0.57 ± 0.06	0.53 ± 0.07
20	0.5 ± 0.04	0.52 ± 0.11	0.54 ± 0.07

279 of the approaches. As shown in the table, subsampling using the proposed framework has
 280 improved the results across all metrics. Note that training the network with a smaller sample
 281 size, when samples are selected using the proposed framework, yields a performance com-
 282 parable to (and even slightly improved over) training the network using the entire training
 283 dataset.

284 The improvement in Recall and F1 Score (marked with an asterisk in Table 2) is statisti-
 285 cally significant when comparing the proposed framework with the random sampling strat-
 286 egy. This improvement has been verified under both Bonferroni and Benjamini-Hochberg
 287 corrections, indicating that the network’s ability to identify positive cases and maintain a
 288 strong precision-recall balance correctly is a statistically reliable improvement. Our pro-
 289 posed subsampling framework demonstrates a consistent, albeit slight, improvement across
 290 most evaluation metrics when compared to training with the complete dataset. Of these
 291 improvements, only the gain in Recall (marked with a double dagger in Table 2) was found
 292 to be statistically significant.

293 **Finding:** The proposed subsampling framework allows for identifying samples that are
 294 more informative in training the network. This approach enables researchers to purposefully
 295 select samples from the dataset, selecting those most helpful for training the networks, rather
 296 than relying on random selection. This is particularly important in utilizing linked datasets,
 297 as it facilitates subsampling for data integration.

298 4. Related Work

299 We can categorize methods for graph subsampling into two main categories: *coreset selection*
 300 and *graph dataset compression*. In this section, we provide a review of methods in each
 301 category and conclude by outlining how our approach differs from these methods.

302 **Coreset selection** is an approach primarily used in active learning to efficiently select
 303 representative samples from an unlabeled dataset for human experts to label (Yoo and
 304 Kweon, 2019). Coreset selection is extensively studied for subsampling purposes, as it
 305 provides methods to identify and sample data points that significantly improve a network’s
 306 learning ability, stemming from the understanding that not all samples contribute equally to
 307 model performance (Katharopoulos and Fleuret, 2018; Jeong et al., 2023; Xie et al., 2023;
 308 Joshi and Mirzasoleiman, 2023; Yoo and Kweon, 2019; Citovsky et al., 2021; Ash et al.,
 309 2020; Caramalau et al., 2021). Principles of coreset selection have been widely applied
 310 to various deep learning domains, including large language models (Xie et al., 2023) and
 311 computer vision (Jeong et al., 2023). However, applying coreset selection to graphs remains
 312 an underexplored topic, particularly for graph subsampling. For instance, Ding et al. (2024)
 313 proposed a method for neighbourhood subgraph selection around a node, which differs from
 314 our focus on selecting graphs for dataset-level subsampling.

Table 2: Results of performance improvement using the proposed framework.

Method	Accuracy	ROC AUC	Precision	Recall	F1 Score
Without Subsampling	0.59 ± 0.07	0.63 ± 0.06	0.59 ± 0.07	0.61 ± 0.1	0.59 ± 0.07
Random Sampling	0.57 ± 0.08	0.59 ± 0.07	0.57 ± 0.08	0.57 ± 0.1	0.57 ± 0.08
Proposed Framework	0.61 ± 0.04	0.63 ± 0.04	0.6 ± 0.05	$0.68 \pm 0.03^{*\dagger}$	$0.64 \pm 0.03^*$

315 There are limited studies on subsampling and coreset selection for graph datasets. The
 316 primary focus of existing graph subsampling studies, such as the KiDD (Xu et al., 2023) and
 317 DosCond (Jin et al., 2022) approaches, is **graph dataset compression**, which involves
 318 compressing the GNN training dataset by creating a synthetic, smaller representation of the
 319 original. Both KiDD and DosCond notably utilize gradient matching for graph compression.
 320 Additionally, MIRAGE (Gupta et al., 2024) further leverages computation trees of training
 321 graphs for dataset compression. Beyond the mentioned studies, researchers have employed
 322 tree mover’s distance (TMD) either to select specific training sets for tasks related to neural
 323 algorithmic reasoning (Georgiev et al., 2023) or to aim to reduce both the number of graphs
 324 and the size of individual graphs for GNN training (Jain et al., 2025). However, this graph
 325 compression paradigm, which prioritizes creating smaller datasets with smaller graphs, is
 326 not ideal for scenarios involving the integration of data from multiple datasets, especially
 327 when the datasets contain a limited number of data points.

328 Our goal is to sample graphs that are most influential in training a GNN for a specific
 329 downstream task, such as graph classification. Our framework will enable researchers to
 330 leverage insights from our subsampling approach to strategically collect more diverse and
 331 potentially multi-source data, facilitating its integration into a unified graph structure that
 332 can improve the network’s performance.

333 5. Conclusion

334 In this paper, we present an efficient framework for data subsampling based on the prediction
 335 uncertainty of the available data points. The purpose of the approach is to help sample
 336 data points from a primary dataset for additional data integration from other available,
 337 and often limited, datasets. The additional data will help augment the primary dataset
 338 and potentially improve network performance. Using the primary dataset, the framework
 339 utilizes self-distillation to quantify the prediction uncertainty of the data points. Using
 340 K-means clustering, the data points are grouped into k clusters based on their graph rep-
 341 resentation. In each cluster, based on the data point’s prediction uncertainty, the data is
 342 grouped into 0-25%, 25-50%, 50-75%, and 75-100% percentiles. Finally, data is sampled
 343 from each cluster with an emphasis on higher percentiles. The evaluations have shown
 344 that when sampling data using the proposed framework, the network trained on the aug-
 345 mented dataset has a statistically significant improvement in performance compared to a
 346 network trained on randomly sampled augmented data. Additionally, the network exhibits
 347 comparable performance to one trained on the whole augmented training dataset.

348 As a future direction, we plan to incorporate explainability into the uncertainty quan-
 349 tification approach to help users better understand the data selection process. Additionally,
 350 we plan to develop an approach to find the right number of samples. Finally, we plan to
 351 evaluate the approach on additional datasets.

352 References

- 353 Jordan T. Ash, Chicheng Zhang, Akshay Krishnamurthy, John Langford, and Alekh Agar-
 354 wal. Deep batch active learning by diverse, uncertain gradient lower bounds. In *Interna-*

- 355 *tional Conference on Learning Representations*, 2020. URL <https://openreview.net/forum?id=ryghZJBKPS>.
- 356
- 357 Razvan Caramalau, Binod Bhattacharai, and Tae-Kyun Kim. Sequential graph convolutional
358 network for active learning. In *Proceedings of the IEEE/CVF Conference on Computer
359 Vision and Pattern Recognition (CVPR)*, pages 9583–9592, June 2021.
- 360 Jiayi Chen, Benteng Ma, Hengfei Cui, and Yong Xia. Think twice before selection: Fed-
361 erated evidential active learning for medical image analysis with domain shifts. In *Pro-
362 ceedings of the IEEE/CVF Conference on Computer Vision and Pattern Recognition
363 (CVPR)*, pages 11439–11449, June 2024.
- 364 Yuzhao Chen, Yatao Bian, Xi Xiao, Yu Rong, Tingyang Xu, and Junzhou Huang. On
365 self-distilling graph neural network, 2021. URL <https://arxiv.org/abs/2011.02255>.
- 366 Gui Citovsky, Giulia DeSalvo, Claudio Gentile, Lazaros Karydas, Anand Rajagopalan, Af-
367 shin Rostamizadeh, and Sanjiv Kumar. Batch active learning at scale. In M. Ranzato,
368 A. Beygelzimer, Y. Dauphin, P.S. Liang, and J. Wortman Vaughan, editors, *Advances
369 in Neural Information Processing Systems*, volume 34, pages 11933–11944. Curran Asso-
370 ciates, Inc., 2021. URL https://proceedings.neurips.cc/paper_files/paper/2021/file/64254db8396e404d9223914a0bd355d2-Paper.pdf.
- 371
- 372 Hirad Daneshvar and Reza Samavi. Gnn’s uncertainty quantification using self-distillation,
373 2025. URL <https://arxiv.org/abs/2506.20046>.
- 374 Mucong Ding, Yinhan He, Jundong Li, and Furong Huang. Spectral greedy coresets for
375 graph neural networks, 2024. URL <https://arxiv.org/abs/2405.17404>.
- 376 Dobrik Georgiev Georgiev, Pietro Lio, Jakub Bachurski, Junhua Chen, Tunan Shi, and
377 Lorenzo Giusti. Beyond erdos-renyi: Generalization in algorithmic reasoning on graphs.
378 In *The Second Learning on Graphs Conference*, 2023. URL <https://openreview.net/forum?id=TTxQAk9QG>.
- 379
- 380 Jianping Gou, Baosheng Yu, Stephen J. Maybank, and Dacheng Tao. Knowledge distil-
381 lation: A survey. *International Journal of Computer Vision*, 129(6):1789–1819, 6 2021.
382 ISSN 1573-1405. doi: 10.1007/s11263-021-01453-z.
- 383 Mridul Gupta, Sahil Manchanda, Hariprasad Kodamana, and Sayan Ranu. Mirage: Model-
384 agnostic graph distillation for graph classification, 2024. URL <https://arxiv.org/abs/2310.09486>.
- 385
- 386 William L Hamilton. Graph representation learning. *Synthesis Lectures on Artificial Intel-
387 ligence and Machine Learning*, 14(3):1–159, 2020.
- 388 Zhexue Huang. Extensions to the k-means algorithm for clustering large data sets with
389 categorical values. *Data Mining and Knowledge Discovery*, 2(3):283–304, 09 1998.
- 390 Mika Sarkin Jain, Stefanie Jegelka, Ishani Karmarkar, Luana Ruiz, and Ellen Vitercik.
391 Subsampling graphs with gnn performance guarantees, 2025. URL <https://arxiv.org/abs/2502.16703>.
- 392

- 393 Yuna Jeong, Myunggwon Hwang, and Wonkyung Sung. Training data selection based on
 394 dataset distillation for rapid deployment in machine-learning workflows. *Multimedia Tools
 395 and Applications*, 82(7):9855–9870, 2023.
- 396 Wei Jin, Xianfeng Tang, Haoming Jiang, Zheng Li, Danqing Zhang, Jiliang Tang, and Bing
 397 Yin. Condensing graphs via one-step gradient matching. In *Proceedings of the 28th ACM
 398 SIGKDD Conference on Knowledge Discovery and Data Mining*, KDD ’22, page 720–730,
 399 New York, NY, USA, 2022. Association for Computing Machinery. ISBN 9781450393850.
 400 doi: 10.1145/3534678.3539429. URL <https://doi.org/10.1145/3534678.3539429>.
- 401 Siddharth Joshi and Baharan Mirzasoleiman. Data-efficient contrastive self-supervised
 402 learning: Most beneficial examples for supervised learning contribute the least. In Andreas Krause,
 403 Emma Brunskill, Kyunghyun Cho, Barbara Engelhardt, Sivan Sabato, and Jonathan Scarlett, editors,
 404 *Proceedings of the 40th International Conference on Machine Learning*, volume 202 of *Proceedings of Machine Learning Research*, pages 15356–15370.
 405 PMLR, 07 2023. URL <https://proceedings.mlr.press/v202/joshi23b.html>.
- 407 Angelos Katharopoulos and Francois Fleuret. Not all samples are created equal: Deep
 408 learning with importance sampling. In Jennifer Dy and Andreas Krause, editors,
 409 *Proceedings of the 35th International Conference on Machine Learning*, volume 80 of
 410 *Proceedings of Machine Learning Research*, pages 2525–2534. PMLR, 07 2018. URL
 411 <https://proceedings.mlr.press/v80/katharopoulos18a.html>.
- 412 James MacQueen. Some methods for classification and analysis of multivariate observations.
 413 In *Proceedings of the Fifth Berkeley Symposium on Mathematical Statistics and
 414 Probability, Volume 1: Statistics*, volume 5, pages 281–298. University of California press,
 415 1967.
- 416 Christopher Morris, Martin Ritzert, Matthias Fey, William L Hamilton, Jan Eric Lenssen,
 417 Gaurav Rattan, and Martin Grohe. Weisfeiler and Leman Go Neural: Higher-order Graph
 418 Neural Networks, 2021.
- 419 Shi Na, Liu Xumin, and Guan Yong. Research on k-means clustering algorithm: An
 420 improved k-means clustering algorithm. In *2010 Third International Symposium on
 421 Intelligent Information Technology and Security Informatics*, pages 63–67, 2010. doi:
 422 10.1109/IITSI.2010.74.
- 423 Burr Settles and Mark Craven. An analysis of active learning strategies for sequence labeling
 424 tasks. In *proceedings of the 2008 conference on empirical methods in natural language
 425 processing*, pages 1070–1079, 2008.
- 426 Sang Michael Xie, Shibani Santurkar, Tengyu Ma, and Percy S Liang. Data se-
 427 lection for language models via importance resampling. In A. Oh, T. Naumann,
 428 A. Globerson, K. Saenko, M. Hardt, and S. Levine, editors, *Advances in Neural
 429 Information Processing Systems*, volume 36, pages 34201–34227. Curran Associates,
 430 Inc., 2023. URL https://proceedings.neurips.cc/paper_files/paper/2023/file/6b9aa8f418bde2840d5f4ab7a02f663b-Paper-Conference.pdf.

- 432 Rui Xu and D. Wunsch. Survey of clustering algorithms. *IEEE Transactions on Neural*
 433 *Networks*, 16(3):645–678, 2005. doi: 10.1109/TNN.2005.845141.
- 434 Zhe Xu, Yuzhong Chen, Menghai Pan, Huiyuan Chen, Mahashweta Das, Hao Yang, and
 435 Hanghang Tong. Kernel ridge regression-based graph dataset distillation. In *Proceedings*
 436 *of the 29th ACM SIGKDD Conference on Knowledge Discovery and Data Mining*, KDD
 437 ’23, page 2850–2861, New York, NY, USA, 2023. Association for Computing Machinery.
 438 ISBN 9798400701030. doi: 10.1145/3580305.3599398. URL <https://doi.org/10.1145/3580305.3599398>.
- 440 Donggeun Yoo and In So Kweon. Learning loss for active learning. In *Proceedings of*
 441 *the IEEE/CVF Conference on Computer Vision and Pattern Recognition (CVPR)*, June
 442 2019.
- 443 Linfeng Zhang, Chenglong Bao, and Kaisheng Ma. Self-distillation: Towards efficient and
 444 compact neural networks. *IEEE Transactions on Pattern Analysis and Machine Intelli-*
 445 *gence*, 44(8):4388–4403, 2022. doi: 10.1109/TPAMI.2021.3067100.

446 Appendix A. Clinical Dataset

447 We utilized two linked datasets, a medical records dataset and a mental health outpatient
 448 questionnaire dataset. Table 3 shows available information in the medical record’s dataset.
 449 The dataset includes several categorical features, which are **triage level**, describing the type
 450 and severity of a patient’s initial symptoms, **visit disposition code**, which indicates how a
 451 patient was discharged from ambulatory care after registration, **service utilization**, which
 452 refers to the specific health professional services accessed during the patient’s visit, and
 453 **most responsible diagnosis code** that identifies the primary, most clinically significant
 454 problem determined by the healthcare provider during service utilization.

455 The patient graph consists of three feature categories: visit (including age, triage, and
 456 disposition), service utilization (based on service code), and diagnosis (using diagnosis code).
 457 Every visit includes at least one diagnosis, and each diagnosis is associated with at least
 458 one service. Connections extracted for each visit are: *visit-visit* (chronologically ordered),
 459 *visit-diagnosis*, and *diagnosis-service*. Figure 3 shows a sample EHR graph.

460 Table 4 shows the subset of the questions used in the mental health questionnaires
 461 dataset. The questions were selected through an ablation study designed to identify the
 462 most influential questions for the downstream task. The question categories have been used
 463 to create nodes and connections between them. We utilized the timeline of events in the
 464 questionnaire to augment the EHR patient graph with the questionnaire responses as shown
 465 in Figure 4.

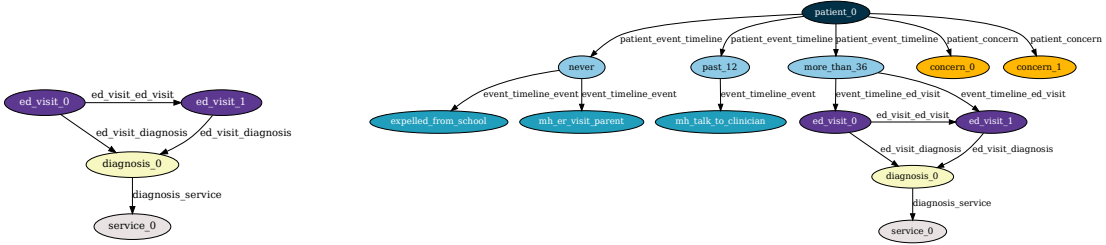


Figure 3: A sample patient graph using EHR data.

Figure 4: A sample augmented patient graph using EHR and questionnaire data.

Table 3: Medical dataset information.

Attribute	Type	Insight	Example
Patient age at the time of visit	Numeric	Min: 4 Max: 17 Mean: 12.5 Std: 3.9	12
ED admission date	Date	Min: 2006-10-16 Max: 2021-07-31	-
Triage level	Categorical	6 Categories	Emergent
Visit disposition code	Categorical	16 Categories	Intra-facility transfer to the ED
Utilized service code	Categorical	35 Categories	Orthopedic Surgery
Diagnosis code	Categorical	707 Categories	Allergic Purpura

Table 4: The subset of selected questionnaires, along with their category.

Question Category	Question
Patient Specific	<p>Are you taking any medication or pills prescribed for mental health concerns?</p> <p>What sex were you assigned at birth, on your original birth certificate?</p> <p>How do you describe yourself (Male, Female, Transgender, Do not identify as female, male or transgender, Don't know)?</p> <p>Are you currently living in a friend's house or apartment?</p> <p>Do you think of yourself as (Straight, Gay or Lesbian, Bisexual, Transgender, transsexual or gender non-conforming, Don't know)?</p> <p>Were you born in Canada?</p>
Events	<p>During the past 12 months, did you visit an emergency room about concerns regarding your mental health?</p> <p>During the past 12 months, have you been suspended or expelled from school?</p> <p>During the past 12 months, did you see or talk to a doctor, psychologist, psychiatrist, or counsellor about concerns regarding your mental health?</p>
Concerns	<p>I am concerned about my physical appearance</p> <p>I am concerned about physically hurting myself</p>